

# Probabilistic Ranking-Aware Ensembles for Enhanced Object Detections

Mingyuan Mao<sup>1</sup>, Baochang Zhang<sup>1,\*</sup>, David Doermann<sup>2</sup>, Jie Guo<sup>1</sup>,  
Shumin Han<sup>3,\*</sup>, Yuan Feng<sup>3</sup>, Xiaodi Wang<sup>3</sup>, Errui Ding<sup>3</sup>

<sup>1</sup>Beihang University, Beijing, China

<sup>2</sup>University at Buffalo, Buffalo, USA

<sup>3</sup>Department of Computer Vision Technology (VIS), Baidu Inc

\*Corresponding author, email: bczhang@buaa.edu.cn, hanshumin@baidu.com

## Abstract

Model ensembles are becoming one of the most effective approaches for improving object detection performance already optimized for a single detector. Conventional methods directly fuse bounding boxes but typically fail to consider proposal qualities when combining detectors. This leads to a new problem of **confidence discrepancy** for the detector ensembles. The confidence has little effect on single detectors but significantly affects detector ensembles. To address this issue, we propose a novel ensemble called the Probabilistic Ranking Aware Ensemble (PRAE) that refines the confidence of bounding boxes from detectors. By simultaneously considering the category and the location on the same validation set, we obtain a more reliable confidence based on statistical probability. We can then rank the detected bounding boxes for assembly. We also introduce a bandit approach to address the confidence imbalance problem caused by the need to deal with different numbers of boxes at different confidence levels. We use our PRAE-based non-maximum suppression (P-NMS) to replace the conventional NMS method in ensemble learning. Experiments on the PASCAL VOC and COCO2017 datasets demonstrate that our PRAE method consistently outperforms state-of-the-art methods by significant margins.

## 1. Introduction

Object detection is one of the hottest topics in the field of computer vision. We have recently witnessed significant success thanks, in part, to the unprecedented representation capacity of Convolutional Neural Networks (CNNs) [48, 21, 20, 59, 56, 58, 38, 44]. In a recent survey [42], the authors categorize numerous approaches to CNN-based object detection as one-stage [59] vs. two-stage [39] architectures, single-scale [59] vs. pyramid feature networks [38], and anchor-based [44] vs. anchor-free [19, 6, 80, 18] tech-

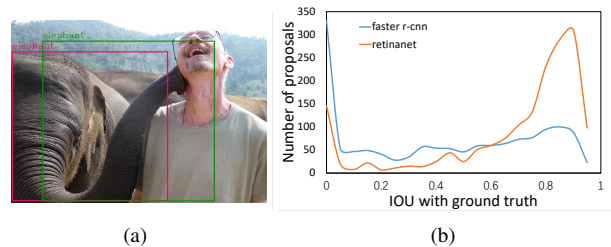


Figure 1. Proposals from different detectors with the same confidence have vastly different localization qualities. a) Faster R-CNN [59] (red) and Retinanet [39] (green) bounding boxes, each with a confidence of 0.7; b) The number of proposals with confidence 0.7 as a function of the IOU with the ground truth on the COCO2017 [41] validation set. (best viewed in color)

niques. These approaches focus on model refinement for a single detector, but their performance is often stifled by their model’s capacity for realistic tasks [74].

As demonstrated by numerous engineering attempts and visual object detection contests [74], single detector approaches still do not perform well enough for real applications. It is our belief, however that detector ensemble approaches can push the boundaries of object detection performance to acceptable levels. Ensembles are also theoretically supported by the fact that when none of the models in an ensemble can detect objects accurately enough, there often exists a combination (ensemble) that can perform better than any individual model. Based on these observations, model ensemble strategies are widely used to meet practical requirements of industrial applications.

Results from object detection models typically include locations (bounding boxes), category labels, and associated confidences. Prevailing ensemble methods in object detection are based on a simple assembly of bounding boxes predicted by the different models. Methods typically use Non-Maximum Suppression (NMS) [51] or Soft-NMS [4] to remove significantly overlap boxes and update box con-

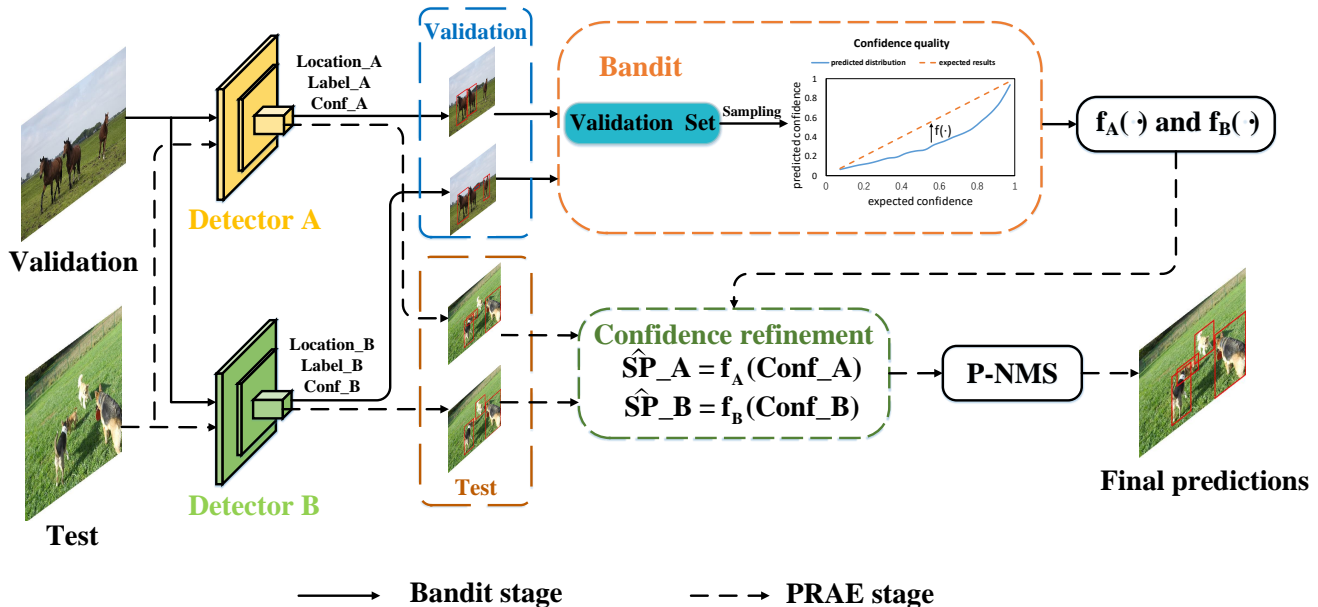


Figure 2. The architecture of the PRAE ensemble.  $f(\cdot)$  represents a mapping relationship between confidence score and statistical probability,  $\hat{SP}$  denotes the refined confidence called statistical probability,  $Conf$  denotes the original predicted confidence, and  $P - NMS$  denotes the PRAE-based NMS. (best viewed in color)

fidences. Following a similar path, Non-maximum weighting (NMW) [82, 53] uses the IOU value to weigh the boxes but does not change the confidence scores. Weighted Boxes Fusion (WBF) [62] refines the bounding box coordinates with significant overlap. They use a voting strategy to compute a weighted average of their locations and tune the weights assigned by different models. The method achieves a good performance but suffers from a tedious parameter tuning process. The weights for the ensemble are greedily traversed over all potential combinations, and this number grows exponentially with the number of models.

Unfortunately, these methods neglect the fact that the proposals from different detectors with the same confidence may have vastly different localization qualities, as shown in Fig. 1. This leads to a **confidence discrepancy problem** (details are given in Section 3.1), which significantly affects the detector ensemble. A possible reason for this is that features extracted by the backbone are shared by the location regressor and classifier in the head [75]. Regression tasks tend to focus on the center point of an object, while classification tasks focus on salient parts [63]. For example, the classification task may consider the head of a person, which is not always at the center of the detection. However, the confidences are mostly category-related. This explains why the proposal qualities are different even for the same confidence. In other words, when the confidence is used to rank the bounding boxes in existing ensemble methods, the

results are less than ideal. While the category-related confidence discrepancy is reduced, we can fairly rank the bounding boxes and eliminate this bottleneck for the ensemble.

In this paper, a probabilistic ranking-aware ensemble (PRAE) method is introduced to refine the confidence score by considering both category and localization information on the same dataset. We first investigate the rationale of the detector ensemble, which shows that different detectors have different proposal qualities. This leads to the confidence discrepancy that generally has little effect on a single detector but significantly affects ensemble detectors. To address this issue, our PRAE refines the predicted confidence by randomly sampling bounding boxes on the same validation dataset, obtaining more reliable confidence called statistical probability. In addition, we introduce the bandit approach (Upper Confidence Bound) to improve the confidence calculation and address the imbalanced confidence problem. Finally, we assemble the refined results and adjust the statistical probability of significantly overlapped bounding boxes using PRAE-based non-maximum suppression (P-NMS). We evaluate various detectors on the PASCAL VOC [15] and COCO2017 [41] datasets to demonstrate the general applicability and effectiveness of our PRAE strategy. Without a tedious parameter tuning process, our algorithm consistently improves the baselines by a large margin. The contributions of this paper are summarized as follows:

1. We are the first, to the best of our knowledge, to

handle the confidence discrepancy problem caused by proposal qualities of different detectors for ensemble models.

2. We present a novel and effective ensemble method called probabilistic ranking-aware ensemble (PRAE), which refines the confidence based on statistical probability by considering both category and localization information on the same dataset.
3. Without tedious parameter tuning, our PRAE method outperforms existing ensemble algorithms by a significant margin.

## 2. Related Work

**Non-maximum suppression (NMS).** Predictions of a detector consist typically of locations (bounding boxes), category labels, and associated confidences. For human detection, Dalal and Triggs [12] demonstrated a greedy NMS algorithm where the bounding box with the maximum detection score is selected, and its neighboring boxes are suppressed using a pre-defined overlap threshold. Since then, NMS has been widely adopted in object detection to reduce the occurrence of false positives. The approach sorts all of the predicted bounding boxes according to their confidence and selects box with the maximum confidence. All other detection boxes with a significant overlap (using a pre-defined threshold) are suppressed. This process is recursively applied to the remaining boxes, and the selected boxes are the final predictions. However, a major issue with NMS is that it sets the score for neighboring detections to zero. Thus, if an object was actually present in that overlap threshold, it would be missed, and this would lead to a reduction in mAP.

**Soft-NMS.** Soft-NMS [4] is proposed to address the issue of missing close detections. Instead of directly suppressing the boxes that are significantly overlapped with the selected box by setting their score to zero, Soft-NMS decreases the detection scores as an increasing function of overlap. Intuitively, if a bounding box has a significant overlap with a box having a higher score, it should take on the higher score, and if the overlap is low, the box can maintain its original score. Soft-NMS give those boxes that would be suppressed during NMS another chance to be selected. Soft-NMS has resulted in noticeable improvements over traditional NMS on standard benchmark datasets, like PASCAL VOC [15] and COCO2017 [41]. However, neither NMS nor Soft-NMS refines the locations of bounding boxes.

**Non-maximum weighting (NMW) and Weighted Boxes Fusion (WBF).** NMW [82, 53] presents that lower confident bounding boxes may consider some latent information that is ignored by the most confident boxes. Especially in the case that two boxes have similar confidences,

predicting the average box is more convincing than directly choosing the higher one. Thus, NMW weighs boxes according to their IOU with the box with the highest confidence, updates the locations by calculating the weighted average of their locations and then implements the NMS method without updating the box confidence. However, NMW does not use information about how many models predict a given box in a cluster and, therefore, does not produce the best results for model ensemble. By contrast, WBF [62] updates a fused box at each step, and uses it to check the overlap with the next predicted boxes. Specifically, it uses confidence scores of all proposed bounding boxes to construct an average box. When several boxes overlap significantly, WBF takes the average of their confidences as the final confidence and takes the weighted average of coordinates as the final location. The strategy improves the quality of the combined predicted bounding boxes and achieves a better mAP than other methods.

However, these methods only focus on the box fusion process and the direct weight assignment for different models but fail to deal with the confidence discrepancy problem before assembly. Besides, for NMW [82, 53] and WBF [62], weights for the ensemble are greedily traversed over all potential combinations, and this number grows exponentially with the number of models. This leads to a tedious parameter tuning process.

## 3. Probabilistic Ranking-Aware Ensembles (PRAE)

In this section, we first describe the confidence discrepancy problem in existing detector ensemble methods. We then present our PRAE method, as shown in Fig. 2 and explain how it works.

### 3.1. Confidence Discrepancies in Detector Ensembles

For object detection, the mAP is the most commonly used evaluation metric. During the inference stage, the results include locations (bounding boxes), category labels, and associated confidences, and the mAP is acquired by sorting the bounding boxes in decreasing order of confidence, obtaining a precision-recall curve, and computing the area bounded by the curves and the axis.

However, we find that sorting bounding boxes in terms of their confidence has two main drawbacks for ensembles. First, the confidence is most often calculated with a normalization strategy using the Softmax function based on a Maximum Entropy Model. Thus, there is typically a deviation from the actual value. Second, the confidence cannot precisely measure the classification and localization quality at the same time, and thus may not be the best sorting criteria for model ensembles.

To address these two issues, we refine the confidence of each bounding box to statistical probability (shortened to  $SP$ ) using our PRAE method. Statistical probability measures the possibility that this bounding box correctly matches a given target object. A correct match requires two conditions. First, the Intersection over Union (IOU) of the bounding box and the target object must be greater than a pre-defined threshold (usually 0.5). Second, the category of the bounding box must be correct. We will show that sorting the  $SP$  value instead of the confidence can achieve higher mAP after ensemble. The detailed calculation of  $SP$  is given in **Section 3.2**.

The  $SP$  value can be roughly estimated by sampling the validation set. We choose several detectors with different mAPs on the COCO2017 validation set [41]. At each confidence level, we compute the ratio of the correct matches to predicted bounding boxes. The results in Fig. 3(a) shows the significant discrepancy between the confidence and the  $SP$  values. More importantly, the discrepancies differ across detectors. One possible reason is that different detectors have different feature extraction capacities. The proposal’s inputs to the classifiers vary in quality, which leads to discrepancies between the confidence and the  $SP$  values shown in Fig. 3(a). In fact, such inconsistencies are one of the most dominant factors that deteriorate ensemble performance.

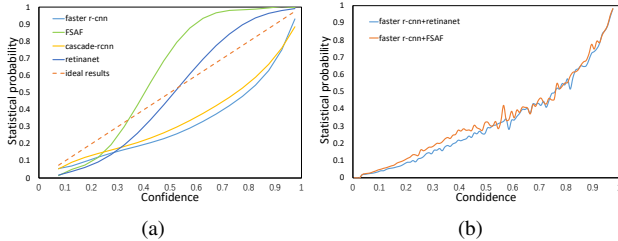


Figure 3. (a) Discrepancies between the confidence and statistical probability of single detectors; (b) discrepancies between the confidence and statistical probability after ensemble. The ensemble method we use is WBF [62].

**Theorem.** *For any predictions (including locations, category labels, and associated confidences), if the ranks of confidence are consistent with ranks of the probability, the expectation of the mAP can be maximized.*

*Proof.* The mAP is defined as the area bounded by the Precision-Recall (PR) curves and axis, which can be approximately calculated as

$$mAP = \frac{1}{N} \sum_{n=1}^N Pr(R_n), \quad (1)$$

and

$$R_n = \frac{1}{N} \times n, \quad (2)$$

situation	$s_m$	$s_n$	prob
1	True	True	$P(s_m)P(s_n)$
2	True	False	$P(s_m)(1 - P(s_n))$
3	False	True	$(1 - P(s_m))P(s_n)$
4	False	False	$(1 - P(s_m))(1 - P(s_n))$

Table 1. Four cases of two predicted boxes. *True* denotes that the predicted box matches a target object, while *False* denotes a false detection.

where  $Pr(R_n)$  represents the corresponding precision value when the recall value equals  $R_n$ , and generally  $N = 100$ . Note that the final mAP is the mean of the result with different IOU thresholds. To facilitate the analysis, Equ. 1 is given based on a specific threshold.

Suppose a certain prediction including locations (bounding boxes), categories, and confidences is denoted as

$$S = \{s_i, i = 1, 2, \dots, N\},$$

and

$$s_i = (bbox_i, conf_i, cls_i).$$

$S$  is sorted based on the confidence from the highest to the lowest.

**A proof by contradiction.** We prove our theorem by contradiction and assume that  $S$  can achieve the highest expectation of mAP, even when the ranks of confidence and probabilities are not consistent. The assumption means that there exists  $m$  and  $n$ , satisfying  $conf_m > conf_n$  and  $prob_m < prob_n$ . Then, we have four possible cases, as shown in Table 1. Then we calculate the expectation of the mAP as

$$E(mAP) = \sum_{i=1}^{N=4} prob_i \times mAP_i, \quad (3)$$

where  $prob_i$  and  $mAP_i$  denote the probability and mAP under the  $i^{th}$  situation. For the ranked box list  $S$ , the predicted boxes are sorted from the highest to the lowest in terms of their confidence, so  $s_m$  ranks higher than  $s_n$ . Thus, we have

$$S_1 = \{s_1, s_2, \dots, s_{m-1}, s_m^T, s_{m+1}, \dots, s_{n-1}, s_n^F, \dots\}, \quad (4)$$

where  $s_m^T$  denotes the  $m^{th}$  box is True, while  $s_n^F$  denotes the  $n^{th}$  box is False, which represents Case 2 in Table 1. Similarly, we have

$$S_2 = \{s_1, s_2, \dots, s_{m-1}, s_m^F, s_{m+1}, \dots, s_{n-1}, s_n^T, \dots\}, \quad (5)$$

which represents Case 3 in Table 1. we define  $S^i$  as

$$S^i = \{s_1, s_2, \dots, s_i\}, \quad (6)$$

Obviously, When  $i \leq m - 1$  or  $i \geq n$ ,  $S_1^i$  and  $S_2^i$  have the same number of *True* and *False* boxes. However, when

$m \leq i \leq n$ , as long as  $S_1^i$  and  $S_2^i$  have the same recall rate  $R_i$ , we have  $P_{r1}(R_i) > P_{r2}(R_i)$ , because  $S_1^i$  always have one less *False* box than  $S_2^i$ . Thus, according to Equ. 1,  $S_1$  achieves higher mAP than  $S_2$  does, and we have  $mAP_2 > mAP_3$ .

Based on the assumption that  $P(s_m) < P(s_n)$  we have  $prob_2 < prob_3$  in Equ. 3. if we appropriately adjust the confidence of  $s_m$  and  $s_n$ , and exchange their positions in  $S$ , and have

$$\hat{S} = \{s_1, s_2, \dots, s_{m-1}, s_n, s_{m+1}, \dots, s_{n-1}, s_m, \dots\}, \quad (7)$$

and then the second and third items in Equ. 3 are changed from

$$S : prob_2 \times mAP_2 + prob_3 \times mAP_3 \quad (8)$$

to

$$\hat{S} : prob_2 \times mAP_3 + prob_3 \times mAP_2. \quad (9)$$

Obviously,  $\hat{S}$  achieves a higher mAP expectation than  $S$ . The **theorem** is proved.  $\square$

**Corollary.** *The bounding boxes' confidences become inconsistent with their probability for ensemble, leading to a sub-optimal detector. The reasons are highlighted in our **theorem**. Only when the sorted bounding boxes maintain a probability consistent with the confidence, a higher mAP can be achieved.*

As shown in Fig. 3(a), there exist obvious confidence discrepancies between detectors. Thus, the confidence of bounding boxes predicted by different detectors has to be refined. We test the conventional ensemble strategy to combine detectors, and the results ( in Fig. 3(b)) show that the confidence and statistical probabilities are significantly inconsistent, which severely deteriorates the ensemble performance. Thus, according to the **theorem**, we introduce the corollary above as a basic principle to improve the performance of the ensemble detector.

### 3.2. Probabilistic Ranking-aware Confidence Refinement

To bridge the gap between the confidence and the probability, we introduce statistical probability as a refined measure of the confidence of each box. We refine the confidence of the bounding boxes based on a validation set shared by all detectors. The result is a fair confidence measure based on statistical probability. The probability that a bounding box correctly matches a target object is a conditional probability, denoted as  $P(box|conf)$ . To estimate  $P(box|conf)$ , we sample on the validation set. We first quantize the original confidence to discrete levels by dividing the confidence interval (0~1) into sub-intervals with a length  $d$  and a centre point defined as

$$c_i = d \times i - \frac{d}{2}, 1 \leq i \leq \text{ceil}(\frac{1}{d}), \quad (10)$$

and the sub-intervals are denoted as

$$l_i = [c_i - \frac{d}{2}, c_i + \frac{d}{2}). \quad (11)$$

In each sub-interval  $l_i$ , we count the number of all bounding boxes  $T_i$  and correct matches  $TP_i$ . We then compute the ratio of  $TP_i$  to  $T_i$  and obtain statistical probability as

$$SP_i = \frac{TP_i}{T_i}, \quad (12)$$

which is a rough estimate of  $P(box|conf)$  in sub-interval  $l_i$ . However,  $T_i$  differs greatly across confidence levels, as shown in Fig. 4, leading to a confidence imbalance problem. Inspired by bandit [2], the number of samples represents the exploitation level. The more samples in a sub-interval  $l_i$ , the more reliable  $SP_i$ . Thus, we introduce Upper Confidence Bound (UCB) to refine  $SP_i$ , which guarantees that every sub-interval is fairly considered as follows:

$$SP_i^* = SP_i + \theta \sqrt{\frac{2 \ln \sum_{i=1}^N T_i}{T_i}}. \quad (13)$$

where  $SP_i^*$  denotes the refined statistical probability in  $l_i$ ,  $\theta$  is a tunable parameter,  $N$  denotes the number of the sub-intervals.

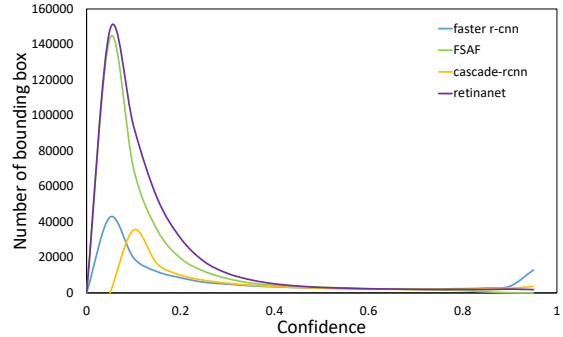


Figure 4. Quantity distribution of bounding boxes across different confidence levels.

However,  $SP^*$  is discrete, which results in quantization error. Obviously, in a certain sub-interval  $l_i$ , it is unfair to transform all confidence values to a single value  $SP_i^*$ , because according to Fig. 3(a), the ranks of the confidence and probability are consistent. This means that the bounding boxes with higher confidences are more likely to locate a target object. Thus, we propose a ranking-aware strategy to further refine the previous  $SP_i^*$  by simultaneously considering the confidence and ranks of bounding boxes. The final statistical probability of the bounding box (denoted as  $\hat{S}P$ ) with the confidence is obtained by

$$\begin{aligned} \hat{S}P_i &= f(\text{confidence}) \\ &= SP_i^* \times \frac{\text{confidence}}{\text{rk}(\text{confidence})}, \end{aligned} \quad (14)$$

and

$$rk(confidence) = \begin{cases} 1, & conf \in l_1, \\ 2, & conf \in l_2, \\ \vdots & \\ N, & conf \in l_N. \end{cases} \quad (15)$$

where  $rk(confidence)$  denotes the rank of the confidence. After probabilistic ranking-aware confidence refinement, the ranks of  $\hat{S}P$  and statistical probability are consistent in the ensemble. This helps to improve the ensemble performance, as suggested by the **theorem in Section 3.1**. Statistical probability achieves confidence refinement globally and guarantees the consistency of confidence and ranks locally, resulting in a more rational indicator for sorting the bounding boxes during evaluation.

### 3.3. PRAE-based NMS (P-NMS)

The overlapping bounding boxes from different detectors are generally handled by an NMS process that directly selects the box with the highest confidence and removes others. However, considering the statistical probability values have reduced the confidence discrepancies between detectors, all overlapping boxes can provide equally important information and should be involved in the calculation. To handle the issue, we introduce a PRAE-based NMS to effectively fuse these overlapping bounding boxes. To do this, when the IOU of several boxes is greater than a threshold, we take the average of their  $\hat{S}P$  values. Then, the location is updated by

$$loc = \sum_{k=1}^n \hat{S}P_k \times loc_k, \quad (16)$$

where  $n$  denotes the number of overlapping boxes,  $\hat{S}P$  and  $loc_k$  denote the refined statistical probability and the location of the  $k^{th}$  bounding box. Note that  $loc$  is a 4-dimensional vector, which contains the co-ordinates of top-left and bottom-right points of the bounding box.

The validation and test set are assumed to be independent identically distributed. As a result,  $\hat{S}P$  obtained on the validation set are also effective on the test set, as verified in **Section 4**. Our PRAE approach is summarized in Algorithm 1.

## 4. Experiments

In this section, we implement our PRAE method to evaluate the effectiveness of the proposed statistical probability. We also compare our method with other state-of-the-art approaches. The performance of the PRAE method is evaluated on various detectors using the PASCAL VOC [15] and COCO2017 [41] datasets.

---

### Algorithm 1 The PRAE method

---

```

# Note: conf is short for confidence
Input: val: validation set.
           $S_A^v$ : Boxes predicted on val by detector A.
           $S_B^v$ : Boxes predicted on val by detector B.
           $S_A^t$ : Boxes predicted on the test set by detector A.
           $S_B^t$ : Boxes predicted by the test set by detector B.
Output:  $S_f$ : Final predictions on the test set.
 $S_f \leftarrow \phi$ 
for  $S$  in  $(S_A^v, S_B^v)$  do
   $c_i, l_i, rk(conf) \leftarrow$  Quantize the confidence interval.
   $SP_i \leftarrow$  Sample on the val.
   $SP_i^* \leftarrow$  Implement bandit.
   $S^t \leftarrow S_A^t$  If  $S$  is  $S_A^v$  Else  $S_B^t$ 
  for  $s$  in  $S^t$  do
     $rk(s) \leftarrow$  based on Equ. 15.
     $\hat{S}P(s) \leftarrow$  based on Equ. 14
     $S_f \leftarrow S_f \cup \hat{S}P(s)$ 
  end for
end for
 $S_f \leftarrow P - NMS(S_f)$ 
Return  $S_f$ 

```

---

### 4.1. Implementation details

To fairly compare with other ensemble methods, we evaluate our PRAE with detectors achieving different mAP levels. For COCO dataset, all selected models are trained on the COCO2017 training set (118k images) and optimized on the validation set (5k images), while for PASCAL VOC dataset, models are trained on VOC07+12 training set (14k images) and optimized on the VOC2007 validation set (2k images).

$d$	0.01	0.03	0.05	0.07
mAP	44.4	45.9	46.1	46.0
$\theta$	0	0.5	1	1.5
mAP	46.1	46.5	46.7	46.5

Table 2. Comparison of different  $d$  in Equ. 10 and  $\theta$  in Equ. 13.  $d$  is set to 0.05 when  $\theta$  varies. mAP denote mAP@(0.5..0.95) on the COCO validation set.

### 4.2. Ablation study

We conduct ablation experiments to evaluate the effect of the parameters. The tunable parameters of the PRAE method are  $d$  in Equ. 10 and  $\theta$  in Equ. 13, which drives the effect of the bandit. We choose FCOS (ResNext101-FPN) [63] with 42.5% mAP and Mask R-CNN (Res2Net101-FPN [86] with 43.6% mAP to ensemble. We vary  $d$  and  $\theta$  separately, and summarize the results evaluated on the COCO2017 validation set in Table 2. To



Model	Retinanet [39] (mAP 37.5)	FCOS [63] (mAP 42.5)	Cascade Mask [5] (mAP 50.3)
	& Faster R-CNN [59] (mAP 39.2)	& Mask R-CNN [24] (mAP 43.6)	& CascadeClsAware (mAP 51.7)
NMS [51]	39.1	44.6	52.6
IOU threshold	0.7	0.65	0.7
weight	[3, 4]	[2, 3]	[1, 2]
Soft-NMS [4]	39.1	44.7	52.3
IOU threshold	0.7	0.7	0.7
sigma	0.1	0.1	0.1
weight	[1, 4]	[4, 5]	[3, 5]
NMW [82, 53]	39.8	45.7	52.8
IOU threshold	0.75	0.7	0.7
weight	[2, 3]	[3, 4]	[1, 2]
WBF [62]	39.0	45.2	52.8
IOU threshold	0.7	0.7	0.7
weight	[1, 4]	[2, 3]	[1, 2]
<b>PRAE (ours)</b>	<b>40.8</b>	<b>46.7</b>	<b>53.4</b>
IOU threshold	0.7	0.7	0.7
weight	[1, 1]	[1, 1]	[1, 1]

Table 3. Ensemble results of two models on the COCO2017 validation set.

confirm the effect of different parts of the PRAE strategy, we conduct another ablation study, as shown in Table 4.

NMS	PRAE	Bandit	P-NMS	mAP@(0.5..0.95) (validation)
✓				44.9
✓	✓			45.5
✓	✓	✓		45.9
	✓	✓	✓	46.7

Table 4. The effects of different parts of the PRAE. The IOU thresholds for NMS and P-NMS are set to 0.7,  $d$  is set to 0.05 and  $\theta$  for bandit is set to 1.

In Table 2, we find that bandit with an appropriate  $\theta$  value plays a positive role in the ensemble. This demonstrates its ability to address the confidence imbalance problem.  $\theta$  is set to 1 in the following experiments. In Table 4, the sorting of the predicted bounding boxes by  $\hat{S}P$  instead of confidence helps to achieve a 0.8% improvement in terms of mAP. This strongly suggests that the proposed statistical probability is a much better indicator of the probability that a bounding box correctly matches a target object than the confidence. Unlike existing methods, P-NMS does not assign tunable weights to different detectors. But it still helps to achieve considerable improvement. This improvement further verifies that PRAE eliminates the confidence discrepancy of detectors, making them equally reliable and thus avoiding the parameter tuning process.

Model	Backbone	$AP_{50}(test)$
Retinanet [39]	ResNet50-FPN	69.8
Faster R-CNN [59]	ResNet50-FPN	71.3
Method	Weight	$AP_{50}(test)$
NMS [51]	[1, 2]	72
Soft-NMS [4]	[2, 3]	72
NMW [82, 53]	[1, 2]	72.1
WBF [62]	[1, 4]	71.1
<b>PRAE (ours)</b>	[1, 1]	<b>73.3</b>

Table 5. Ensemble results of two models on the Pascal VOC2007 test set.

### 4.3. An Ensemble of two models

Existing ensemble methods need to weigh different models before assembling them. The ensemble performance is very sensitive to the pre-defined weights. To eliminate the effects of these weights as much as possible, we implement an ensemble of only two models to fairly compare our PRAE method. We test our PRAE method on the PASCAL VOC2007 [15] test set and the COCO2017 [41] validation set.

For the VOC dataset, we choose Faster R-CNN [59] (ResNet50-FPN as a backbone and 1x training schedule) and Retinanet [39] (ResNet50-FPN as a backbone and 1x training schedule) for ensemble. The results are shown in Table 5.

For the COCO dataset, we select three groups of detectors with low, medium, and high mAP scores. In the low-mAP group, we choose Retinanet [39] with 37.5 mAP

Model	Backbone	Lr schd	$AP$	$AP_{50}$	$AP_{75}$	$AP_S$	$AP_M$	$AP_L$
FCOS [63]	ResNext-101-FPN	2x	43.1	62.8	46.3	26.1	45.7	53.4
Mask R-CNN	Res2Net101-FPN	2x	45.3	65.1	50.0	26.8	48.7	57.0
HTC [8]	Res2Net101-FPN	20e	47.9	67.2	52.3	28.2	51.0	60.6
Cascade Mask	SENet154-vd-FPN	1.44x	50.7	69.6	55.2	31.1	53.4	65.0
CascadeClsAware Faster	ResNet200-vd-FPN	2.5x	52.1	70.0	57.4	34.2	54.4	64.0
Cascade Faster	CBResNet200-vd-FPN	2.5x	53.8	71.8	59.4	35.7	56.4	66.4
Method	Weight	IOU threshold	$AP$	$AP_{50}$	$AP_{75}$	$AP_S$	$AP_M$	$AP_L$
NMS [51]	[1, 3, 4, 7, 8, 9],	0.65	54.3	72.7	60.1	36	57.1	67.2
	[1, 1, 1, 1, 1, 1]	0.65	51.5	70.7	57.4	33.8	54.8	64.1
Soft-NMS [4]	[1, 3, 4, 7, 8, 9]	0.65	53.9	72.6	58.9	35.5	56.4	66.6
	[1, 1, 1, 1, 1, 1]	0.65	50.8	70.7	56	33.2	53.9	63.4
NMW [82, 53]	[2, 3, 5, 7, 8, 9]	0.7	54.6	73.0	61.3	36.9	57.9	67.1
	[1, 1, 1, 1, 1, 1]	0.65	53.4	71.3	59.6	35.4	56.9	66.1
WBF [62]	[2, 4, 5, 7, 8, 9]	0.7	54.7	73.1	61.5	37.4	57.8	67.0
	[1, 1, 1, 1, 1, 1]	0.7	52.7	72.4	58.9	36.0	55.9	64.1
<b>PRAE (ours)</b>	[1, 1, 1, 1, 1, 1]	0.7	<b>56.0</b>	<b>73.8</b>	<b>61.9</b>	<b>37.6</b>	<b>58.6</b>	<b>68.3</b>

Table 6. Ensemble results of multiple models of COCO2017 test-dev set. Red parts show the performance of existing methods without weight tuning.

(ResNet50-FPN as a backbone and 2x training schedule), and Faster R-CNN [59] with 39.2 mAP (ResNet50-FPN as a backbone and 2x training schedule). In the medium-mAP group, we choose FCOS [63] with 42.5 mAP (ResNext-101-FPN as a backbone and 2x training schedule) and Mask R-CNN [24] (Res2Net101-FPN as a backbone and 2x training schedule) with 43.6 mAP. In the high-mAP group, we choose Cascade Mask (SENet154-vd-FPN as a backbone and 1.44x training schedule) with 50.3 mAP, and CascadeClsAware (ResNet200-vd-FPN-Nonlocal as a backbone and 2.5x training schedule) with 51.7 mAP. The results are shown in Table 3.

The results indicate that without tedious parameter tuning, the proposed PRAE method consistently outperforms existing methods by significant margins. Furthermore, the PRAE is effective across different mAP levels and different datasets, which proves its general applicability and effectiveness.

#### 4.4. An ensemble of multiple models

We also combine the results of multiple models to verify the efficiency of our method. Specifically, we choose FCOS [63], Mask R-CNN [24], and several improved versions of Cascade R-CNN [5]. These models include one-stage and two-stage detectors with different mAP level, which makes the comparison more convincing. The parameters are optimized on the COCO2017 [41] validation set, and methods are evaluated on the test-dev set. The results in Table 6 show that the performance of existing methods is very sensitive to the weight assignment. When assigning equal weight to every model, the ensemble performance of

existing methods is severely deteriorated, as the confidence discrepancies of different models are inconsistent. Thus parameter tuning is indispensable for them. However, the combination of weights tends to grow exponentially with the number of models, which becomes unacceptable. By contrast, by bridging the gap between the confidence and the probability, without tedious parameter tuning, PRAE methods still outperform all baselines and advance the state-of-the-art for ensemble methods significantly. The per-class performance is provided in the supplementary materials.

We also compare our PRAE with other methods when there is a huge domain gap between the validation set and test set, which shows that the PRAE still outperforms other methods (provided in supplementary materials).

## 5. Conclusion

We have proposed an elegant and effective approach, referred to as the Probabilistic Ranking Aware Ensembles (PRAE) method, for visual object detection. The proposed statistical probability refine the predicted confidence by randomly sampling bounding boxes on the same validation dataset, obtaining more reliable confidence, and thus achieve a more rational indicator to measure the qualities of bounding boxes. With PRAE implemented, we have significantly improved the performance of the model ensemble, in contrast to the baselines and the state-of-the-art methods. The underlying effect is that PRAE bridges the gap between the confidence and the probability, and thus addressing the confidence discrepancy issue of detectors, which leads to improved ensemble results. Our PRAE method provides fresh insight into model ensembles for object detection.



## References

- [1] <https://github.com/PaddlePaddle/PaddleDetection>.
- [2] P. Auer, N. Cesa-Bianchi, Y. Freund, and R. E. Schapire. Gambling in a rigged casino: The adversarial multi-armed bandit problem. In *Proceedings of IEEE 36th Annual Foundations of Computer Science*, pages 322–331, 1995.
- [3] Chandrasekhar Bhagavatula, Chenchen Zhu, Khoa Luu, and Marios Savvides. Faster than real-time facial alignment: A 3d spatial transformer network approach in unconstrained poses. In *IEEE ICCV*, pages 3980–3989, 2017.
- [4] Navaneeth Bodla, Bharat Singh, Rama Chellappa, and Larry S. Davis. Improving object detection with one line of code. In *ICCV*, 2017.
- [5] Zhaowei Cai and Nuno Vasconcelos. Cascade r-cnn: Delving into high quality object detection. In *IEEE CVPR*, pages 6154–6162, 2018.
- [6] Nicolas Carion, Francisco Massa, Gabriel Synnaeve, Nicolas Usunier, Alexander Kirillov, and Sergey Zagoruyko. End-to-end object detection with transformers. *arXiv:2005.12872*, 2020.
- [7] Chaoqi Chen, Zebiao Zheng, Xinghao Ding, Yue Huang, and Qi Dou. Harmonizing transferability and discriminability for adapting object detectors. In *IEEE CVPR*, 2020.
- [8] Kai Chen, Jiangmiao Pang, Jiaqi Wang, Yu Xiong, , and Xiaoxiao Li et al. Hybrid task cascade for instance segmentation. In *CVPR*, 2019.
- [9] Kai Chen, Jiaqi Wang, Jiangmiao Pang, Yuhang Cao, Yu Xiong, Xiaoxiao Li, Shuyang Sun, Wansen Feng, Ziwei Liu, Jiarui Xu, Zheng Zhang, Dazhi Cheng, Chenchen Zhu, Tianheng Cheng, Qijie Zhao, Buyu Li, Xin Lu, Rui Zhu, Yue Wu, Jifeng Dai, Jingdong Wang, Jianping Shi, Wanli Ouyang, Chen Change Loy, and Dahua Lin. MMDetection: Open mmlab detection toolbox and benchmark. *arXiv:1906.07155*, 2019.
- [10] Jiwoong Choi, Dayoung Chun, Hyun Kim, and Hyuk-Jae Lee. Gaussian yolov3: An accurate and fast object detector using localization uncertainty for autonomous driving. In *IEEE ICCV*, pages 502–511, 2019.
- [11] Jifeng Dai, Haozhi Qi, Yuwen Xiong, Yi Li, Guodong Zhang, Han Hu, and Yichen Wei. Deformable convolutional networks. In *IEEE ICCV*, page 764–773, 2017.
- [12] N. Dalal and B. Triggs. Histograms of oriented gradients for human detection. In *IEEE CVPR*, volume 1, pages 886–893, 2005.
- [13] Piotr Dollár. Pedestrian detection: A benchmark. In *IEEE CVPR*, pages 304–311, 2019.
- [14] Kaiwen Duan, Song Bai, Lingxi Xie, Honggang Qi, Qingming Huang, and Qi Tian. Centernet: Object detection with keypoint triplets. In *IEEE CVPR*, 2019.
- [15] Mark Everingham, Luc Van Gool, Christopher K. I. Williams, John Winn, and Andrew Zisserman. The pascal visual object classes (voc) challenge. In *IJCV*, pages 303–338, 2015.
- [16] Ronald A Fisher. On the mathematical foundations of theoretical statistics. *Philosophical Transactions of the Royal Society of London. Series A, Containing Papers of a Mathematical or Physical Character*, 222(594-604):309–368, 1922.
- [17] Cheng-Yang Fu, Wei Liu, Ananth Ranga, Amrith Tyagi, and Alexander C. Berg. DSSD: Deconvolutional single shot detector. In *arXiv preprint arXiv:1701.06659*.
- [18] Peng Gao, Minghang Zheng, Xiaogang Wang, Jifeng Dai, and Hongsheng Li. Fast convergence of DETR with spatially modulated co-attention. *arXiv:2101.07448*, 2021.
- [19] Golnaz Ghiasi, Tsung-Yi Lin, and Quoc V. Le. NAS-FPN: learning scalable feature pyramid architecture for object detection. In *IEEE CVPR*, pages 7036–7045, 2019.
- [20] Ross B. Girshick. Fast R-CNN. In *IEEE ICCV*, pages 1440–1448, 2015.
- [21] Ross B. Girshick, Jeff Donahue, Trevor Darrell, and Jitendra Malik. Rich feature hierarchies for accurate object detection and semantic segmentation. In *IEEE CVPR*, pages 580–587, 2014.
- [22] Priya Goyal, Piotr Dollár, Ross Girshick, Pieter Noordhuis, Lukasz Wesolowski, Aapo Kyrola, Andrew Tulloch, Yangqing Jia, and Kaiming He. Accurate, large minibatch sgd: training imagenet in 1 hour. *arXiv: 1706.02677*, 2017.
- [23] C. Harris and M. Stephens. A combined corner and edge detector. *Alvey vision conference*, 15:10–5244, 1988.
- [24] Kaiming He, Georgia Gkioxari, Piotr Dollár, and Ross B. Girshick. Mask R-CNN. In *IEEE ICCV*, pages 2980–2988, 2017.
- [25] Kaiming He, Xiangyu Zhang, Shaoqing Ren, and Jian Sun. Deep residual learning for image recognition. In *IEEE CVPR*, pages 770–778, 2016.
- [26] Yihui He, Xiaobo Ma, Xiapu Luo, Jianfeng Li, Mengchen Zhao, Bo An, and Xiaohong Guan. Vehicle traffic driven camera placement for better metropolis security surveillance. *IEEE Intelligent Systems*, PP(99):1–1, 2017.
- [27] Yihui He, Chenchen Zhu, Jianren Wang, Marios Savvides, and Xiangyu Zhang. Bounding box regression with uncertainty for accurate object detection. *arXiv:1809.08545*, 2018.
- [28] Isaac Horowitz. Fundamental theory of automatic linear feedback control systems. *IRE Transactions on Automatic Control*, 4(3):5–19, 1959.
- [29] Han Hu, Jiayuan Gu, Zheng Zhang, Jifeng Dai, and Yichen Wei. Relation networks for object detection. In *IEEE CVPR*, pages 3588–3597, 2018.
- [30] Zeyi Huang, Wei Ke, and Dong Huang. Improving object detection with inverted attention. *arXiv:1903.12255*, 2019.
- [31] Borui Jiang, Ruixuan Luo, Jiayuan Mao, Tete Xiao, and Yuning Jiang. Acquisition of localization confidence for accurate object detection. In *ECCV*, pages 784–799, 2018.
- [32] Tao Kong, Fuchun Sun, Huaping Liu, Yuning Jiang, and Jianbo Shi. Foveabox: Beyond anchor-based object detector. *arXiv:1904.03797*, 2019.
- [33] Hei Law and Jia Deng. Cornernet: Detecting objects as paired keypoints. In *ECCV*, pages 765–781, 2018.
- [34] Breiman Leo. Bagging predictors. *Machine Learning*, 24(2):123–140, 1996.
- [35] Yanghao Li, Yuntao Chen, Naiyan Wang, and Zhaoxiang Zhang. Scale-aware trident networks for object detection. In *IEEE ICCV*, pages 502–511, 2019.

- [36] Yu Li, Tao Wang, Bingyi Kang, Sheng Tang, Chunfeng Wang, Jintao Li, and Jiashi Feng. Overcoming classifier imbalance for long-tail object detection with balanced group softmax. In *IEEE CVPR*, 2020.
- [37] Xiaodan Liang, Tairui Wang, Luona Yang, and Eric Xing. Cirl: Controllable imitative reinforcement learning for vision-based self-driving. In *ECCV*, pages 584–599, 2018.
- [38] Tsung-Yi Lin, Piotr Dollár, Ross B. Girshick, Kaiming He, Bharath Hariharan, and Serge J. Belongie. Feature pyramid networks for object detection. In *IEEE CVPR*, pages 936–944, 2017.
- [39] Tsung-Yi Lin, Priya Goyal, Ross B. Girshick, Kaiming He, and Piotr Dollár. Focal loss for dense object detection. In *IEEE ICCV*, pages 2999–3007, 2017.
- [40] Tsung-Yi Lin, Michael Maire, Serge J. Belongie, James Hays, Pietro Perona, Deva Ramanan, Piotr Dollár, and C. Lawrence Zitnick. Microsoft COCO: common objects in context. In *ECCV*, 2014.
- [41] Tsung-Yi Lin, Michael Maire, Serge J. Belongie, Lubomir D. Bourdev, Ross B. Girshick, James Hays, Pietro Perona, Deva Ramanan, Piotr Dollár, and C. Lawrence Zitnick. Microsoft coco: Common objects in context. In *ECCV*, pages 740–755, 2014.
- [42] Li Liu, Wanli Ouyang, Xiaogang Wang, Paul Fieguth, Jie Chen, Xinwang Liu, and Matti Pietikainen. Deep learning for generic object detection: A survey. *Int. J. Comp. Vis.*, 2019.
- [43] Songtao Liu, Di Huang, and Yunhong Wang. Receptive field block net for accurate and fast object detection. In *ECCV*, pages 385–400, 2018.
- [44] Wei Liu, Dragomir Anguelov, Dumitru Erhan, Christian Szegedy, Scott E. Reed, Cheng-Yang Fu, and Alexander C. Berg. SSD: single shot multibox detector. In *ECCV*, pages 21–37, 2016.
- [45] Jonathan Long, Evan Shelhamer, and Trevor Darrell. Fully convolutional networks for semantic segmentation. In *IEEE CVPR*, pages 3431–3440, 2015.
- [46] Xin Lu, Buyu Li, Yuxin Yue, Quanquan Li, and Junjie Yan. Grid R-CNN. In *IEEE CVPR*, 2019.
- [47] A. M. Lyapunov and J. A. Walker. The general problem of the stability of motion. *Journal of Applied Mechanics*, 61(1):226, 1892.
- [48] Mingyuan Mao, Yuxin Tian, Baochang Zhang, Qixiang Ye, Wanquan Liu, Guodong Guo, and David Doermann. iffDetector: Inference-aware feature filtering for object detection. In *arXiv preprint arXiv:2006.12708*.
- [49] Oded Maron and Tomás Lozano-Pérez. A framework for multiple-instance learning. In *NeurIPS*, pages 570–576, 1997.
- [50] Francisco Massa and Ross Girshick. Maskrcnn-benchmark: Fast, ModularPreference Implementation of Instance Segmentation and Object Detection algorithms in PyTorch. <https://github.com/facebookresearch/maskrcnn-benchmark>, 2018. Accessed: [2018-11-16].
- [51] A Neubeck and L Van Gool. Efficient non-maximum suppression. In *ICPR*, pages 850–855, 2006.
- [52] Alejandro Newell, Kaiyu Yang, and Jia Deng. Stacked hour-glass networks for human pose estimation. In *ECCV*, pages 483–499, 2016.
- [53] Chengcheng Ning, Huajun Zhou, Yan Song, and Jinhui Tang. Inception single shot multibox detector for object detection. In *ICMEW*, 2017.
- [54] Junran Peng, Ming Sun, Zhaoxiang Zhang, Tieniu Tan, and Junjie Yan. Pod: Practical object detection with scale-sensitive network. In *IEEE ICCV*, pages 6054–6063, 2019.
- [55] Qi Qian, Lei Chen, Hao Li, and Rong Jin. Dr loss: Improving object detection by distributional ranking. In *IEEE CVPR*, 2020.
- [56] Joseph Redmon, Santosh Kumar Divvala, Ross B. Girshick, and Ali Farhadi. You only look once: Unified, real-time object detection. In *IEEE CVPR*, pages 779–788, 2016.
- [57] Joseph Redmon and Ali Farhadi. YOLO9000: better, faster, stronger. In *IEEE CVPR*, pages 6517–6525, 2017.
- [58] Joseph Redmon and Ali Farhadi. Yolov3: An incremental improvement. *arXiv: 1804.02767*, 2018.
- [59] Shaoqing Ren, Kaiming He, Ross B. Girshick, and Jian Sun. Faster R-CNN: towards real-time object detection with region proposal networks. In *NeurIPS*, pages 91–99, 2015.
- [60] A. Rosenfeld and M. Thurston. Edge and curve detection for visual scene analysis. *IEEE Transactions on computers*, 100(5):562–569, 1971.
- [61] Abhinav Shrivastava, Rahul Sukthankar, Jitendra Malik, and Abhinav Gupta. Beyond skip connections: Top-down modulation for object detection. *arXiv:1612.06851*, 2016.
- [62] Roman Solovyev, Weimin Wang, and Tatiana Gabruseva. Weighted boxes fusion: ensembling boxes for object detection models.
- [63] Zhi Tian, Chunhua Shen, Hao Chen, and Tong He. Fcos: Fully convolutional one-stage object detection. *arXiv:1904.01355*, 2019.
- [64] P. Viola and M. Jones. Rapid object detection using a boosted cascade of simple features. In *IEEE CVPR*, volume 1, pages 1–1, 2001.
- [65] P. Viola and M. Jones. Rapid object detection using a boosted cascade of simple features. In *Proceedings of the 2001 IEEE Computer Society Conference on Computer Vision and Pattern Recognition. CVPR 2001*, volume 1, pages I–I, 2001.
- [66] Fang Wan, Chang Liu, Wei Ke, Xiangyang Ji, Jianbin Jiao, and Qixiang Ye. C-MIL: continuation multiple instance learning for weakly supervised object detection. In *IEEE CVPR*, pages 2199–2208, 2019.
- [67] Fang Wan, Pengxu Wei, Zhenjun Han, Jianbin Jiao, and Qixiang Ye. Min-entropy latent model for weakly supervised object detection. *IEEE Trans. Pattern Anal. Mach. Intell.*, 41(10):2395–2409, 2019.
- [68] Jiaqi Wang, Kai Chen, Shuo Yang, Chen Change Loy, and Dahua Lin. Region proposal by guided anchoring. In *IEEE CVPR*, pages 2965–2974, 2019.
- [69] Xiaolong Wang and Abhinav Gupta. Videos as space-time region graphs. In *ECCV*, pages 399–417, 2018.
- [70] Saining Xie, Ross Girshick, Piotr Dollar, Zhuowen Tu, and Kaiming He. Aggregated residual transformations for deep neural networks. In *IEEE CVPR*, pages 1492–1500, 2017.

- [71] Tong Yang, Xiangyu Zhang, Zeming Li, Wenqiang Zhang, and Jian Sun. Metaanchor: Learning to detect objects with customized anchors. In *NeurIPS*, pages 320–330, 2018.
- [72] Ze Yang, Shaohui Liu, Han Hu, Liwei Wang, and Stephen Lin. Reppoints: Point set representation for object detection. In *IEEE ICCV*, pages 502–511, 2019.
- [73] Jiahui Yu, Yuning Jiang, Zhangyang Wang, Zhimin Cao, and Thomas S. Huang. Unitbox: An advanced object detection network. In *ACM Multimedia Conference*, pages 516–520, 2016.
- [74] Xuehui Yu, Zhenjun Han, Yuqi Gong, Nan Jan, Jian Zhao, and Qixiang Ye et al. The 1st tiny object detection challenge: Methods and results. *CoRR*, abs/2009.07506, 2020.
- [75] Yuhang Zang Yan Gao Enze Xie Junjie Yan Chen Change Loy Xiaogang Wang. Yu Liu, Guanglu Song. 1st place solutions for openimage2019 – object detection and instance segmentation.
- [76] Lu Yuan Zicheng Liu Lijuan Wang Hongzhi Li Yue Wu, Yinpeng Chen and Yun Fu. Rethinking classification and localization for object detection. In *IEEE CVPR*, 2020.
- [77] Shifeng Zhang, Cheng Chi, Yongqiang Yao, Zhen Lei, and Stan Z. Li. Bridging the gap between anchor-based and anchor-free detection via adaptive training sample selection. In *IEEE CVPR*, 2020.
- [78] Shifeng Zhang, Longyin Wen, Xiao Bian, Zhen Lei, and Stan Z. Li. Single-shot refinement neural network for object detection. In *IEEE CVPR*, pages 4203–4212, 2018.
- [79] Xiaosong Zhang, Fang Wan, Chang Liu, Rongrong Ji, and Qixiang Ye. FreeAnchor: Learning to match anchors for visual object detection. In *NeurIPS*, 2019.
- [80] Minghang Zheng, Peng Gao, Xiaogang Wang, Hongsheng Li, and Hao Dong. End-to-end object detection with adaptive clustering transformer. *arXiv:2011.09315*, 2020.
- [81] Yutong Zheng, Dipan K. Pal, and Marios Savvides. Ring loss: Convex feature normalization for face recognition. In *IEEE CVPR*, pages 5089–5097, 2018.
- [82] Huajun Zhou, Zechao Li, Chengcheng Ning, and Jinhui Tang. Cad: Scale invariant framework for real-time object detection. In *ICCVW*, 2017.
- [83] Xinyu Zhou, Cong Yao, He Wen, Yuzhi Wang, Shuchang Zhou, Weiran He, and Jiajun Liang. EAST: an efficient and accurate scene text detector. In *IEEE CVPR*, pages 2642–2651, 2017.
- [84] Xingyi Zhou, Jiacheng Zhuo, and Philipp Krähenbühl. Bottom-up object detection by grouping extreme and center points. In *IEEE CVPR*, pages 850–859, 2019.
- [85] Chenchen Zhu, Fangyi Chen, Zhiqiang Shen, and Marios Savvides. Soft anchor-point object detection. In *ECCV*, 2020.
- [86] Chenchen Zhu, Yihui He, and Marios Savvides. Feature selective anchor-free module for single-shot object detection. In *IEEE CVPR*, pages 840–849, 2019.
- [87] Chenchen Zhu, Ran Tao, Khoa Luu, and Marios Savvides. Seeing small faces from robust anchor’s perspective. In *IEEE CVPR*, pages 5127–5136, 2018.